https://doi.org/10.5607/en23039
Exp Neurobiol. 2023 Dec;32(6):395-409.
pISSN 1226-2560 • eISSN 2093-8144

Original Article

Experimental Neurobiology

Mapping Astrocytic and Neuronal μ-opioid Receptor Expression in Various Brain Regions Using MOR-mCherry Reporter Mouse

Woojin Won[1†], Daeun Kim[1,2†], Eunjin Shin[1] and C. Justin Lee[1*]

[1]Center for Cognition and Sociality, Institute for Basic Science (IBS), Daejeon 34126, [2]Department of Biomedical Engineering, College of Information and Biotechnology, Ulsan National Institute of Science and Technology (UNIST), Ulsan 44919, Korea

The μ-opioid receptor (MOR) is a class of opioid receptors characterized by a high affinity for β-endorphin and morphine. MOR is a G protein-coupled receptor (GPCR) that plays a role in reward and analgesic effects. While expression of MOR has been well established in neurons and microglia, astrocytic MOR expression has been less clear. Recently, we have reported that MOR is expressed in hippocampal astrocytes, and its activation has a critical role in the establishment of conditioned place preference. Despite this critical role, the expression and function of astrocytic MOR from other brain regions are still unknown. Here, we report that MOR is significantly expressed in astrocytes and GABAergic neurons from various brain regions including the hippocampus, nucleus accumbens, periaqueductal gray, amygdala, and arcuate nucleus. Using the MOR-mCherry reporter mice and Imaris analysis, we demonstrate that astrocytic MOR expression exceeded 60% in all tested regions. Also, we observed similar MOR expression of GABAergic neurons as shown in the previous distribution studies and it is noteworthy that MOR expression is particularly in parvalbumin (PV)-positive neurons. Furthermore, consistent with the normal MOR function observed in the MOR-mCherry mouse, our study also demonstrates intact MOR functionality in astrocytes through iGluSnFr-mediated glutamate imaging. Finally, we show the sex-difference in the expression pattern of MOR in PV-positive neurons, but not in the GABAergic neurons and astrocytes. Taken together, our findings highlight a substantial astrocytic MOR presence across various brain regions.

Key words: Astrocytes, Mu-opioid receptor, Mapping, Sex-difference

INTRODUCTION

μ-opioid receptor (MOR) is one of the opioid receptors that is an inhibitory $G\alpha_i$- protein-coupled receptor (Gi-GPCR) [1, 2]. MOR is widely distributed in the central nervous system, such as the nucleus accumbens, hippocampus, amygdala, periaqueductal gray, and spinal cord, where it plays a major role in pain, addiction, reward, and motivation [2]. MOR has a high affinity for substances including morphine, β-endorphin, and enkephalin, and is thought to be expressed primarily on GABAergic inhibitory neurons to disinhibit neighboring principal neurons [3].

While most research on MOR has focused on its expression and function in GABAergic inhibitory neurons, recent studies have highlighted the expression and role of MOR in astrocytes [3-5]. It has been demonstrated through experiments using MOR knockout mice and shRNA-mediated MOR knockdown that astrocytic MOR in the hippocampus induces glutamate release [4-6]. Notably, activation of astrocytic MOR leads to glutamate release through TREK-1-containing K2P channels, enhancing synaptic transmission and plasticity in the hippocampus [5, 7]. Despite this novel signaling pathway of MOR in astrocytes, there is a lack of comprehensive mapping and quantification of astrocytic MOR in the brain.

In addition, recent studies highlighted that opioid receptors exhibit sex and age differences in various brain regions, including the

Submitted December 9, 2023, Revised December 23, 2023,
Accepted December 27, 2023

*To whom correspondence should be addressed.
TEL: 82-42-878-9150, FAX: 82-42-878-9151
e-mail: cjl@ibs.re.kr
†These authors contributed equally to this article.

hippocampus, arcuate nucleus, and amygdala [8-10]. Stress and gonadal hormones affect the protein expression and trafficking of MOR in parvalbumin (PV) neurons in the hippocampus [8, 9]. Also, MOR binding density is higher in juveniles than in adults, with potential implications for reward and drug-seeking behaviors [11]. In the amygdala, males have greater delta opioid receptor immunoreactivity than females [12]. Similarly, estrogen treatment has been found to increase MOR mRNA levels in the arcuate nucleus in female rats [13]. These findings collectively suggest that sex-differences in MOR expression may play a role in modulating reproductive behaviors, social behaviors, and stress responses. However, these studies on sexual dimorphism in MOR have only focused on GABAergic neurons, but not on astrocytes.

The *Oprm1*^{tm4Kff} reporter mouse line (MOR-mCherry) [14-16], in which mCherry is tagged to the C-terminus of MOR, has been widely utilized to investigate MOR expression in neurons, due to the advantages of the unique transgenic property. Furthermore, this mouse line has confirmed the remaining functional MOR characteristics in MOR-mCherry mice, including normal *Oprm1* gene transcription, proper distribution and trafficking of MOR-mCherry, comparable MOR agonist binding and potency, and conditioned place preference and pain-related behavioral responses as similar as observed in the wild-type mouse (*Oprm1*$^{+/+}$) [14]. Although we have previously demonstrated the co-expression of MOR with TREK-1 in the hippocampal astrocytes in MOR-mCherry mice, the comprehensive mapping, quantification, and functionality of astrocytic MOR in MOR-mCherry mice has not been investigated.

In this study, we aimed to map MOR-mCherry signal expression in astrocytes across the various brain regions including the hippocampus, nucleus accumbens, periaqueductal gray, amygdala, and arcuate nucleus, and compare it with MOR-mCherry expression in GABAergic neurons and PV-positive neurons. We also confirmed that MOR is fully functional in hippocampal astrocytes in MOR-mCherry mice. Finally, we investigated the sex-dependent expression of MOR-mCherry that might be relevant to the sexual dimorphism of MOR expression in the various brain regions.

MATERIALS AND METHODS

Animals

All MOR-mCherry reporter mice (*Oprm1*^{tm4Kff}; Jackson Laboratories; Stock No. 029013) [14] were group-housed in a humidity and temperature-controlled environment with a 12 h light/dark cycle (8:00 AM~8:00 PM) and had free access to food and water. All animal care and handling were followed by the Institutional Animal Care and Use Committee of the Institute for Basic Science (Approval no. IBS-2023-03-13).

Immunohistochemistry

Animals were deeply anesthetized using isoflurane and perfused with 0.9% saline, followed by 4% paraformaldehyde. Brains were post-fixed in 4% paraformaldehyde at 4°C for 24 h and dehydrated in 30% sucrose at 4°C for 24 h. Brains were then cut in a coronal section of 30 μm on a cryosection. Sections were blocked in 0.1 M PBS containing 0.3% Triton X-100 (Sigma) and 2% donkey serum (Genetex) and 2% goat serum (abcam) for 1.5 h at room temperature. The primary antibodies used were as follows: rabbit anti-S100β (1:200, ab52642, abcam), guineapig anti-GABA (1:500, ab175, abcam), and guineapig anti-PV (1:200, 195 004, Synaptic systems). Samples with primary antibodies were incubated overnight at 4°C. The samples were then washed three times in 0.1 M PBS and incubated with appropriate secondary antibodies (1:500) from Jackson Laboratory for 1.5 h. After three rinses in 0.1 M PBS, the samples were mounted on a Polysine microscopic slide glass (Thermo Scientific). Images were acquired using a Zeiss LSM 900 microscope.

The super-resolution images were obtained using the Elyra 7 super-resolution microscope and processed using ZEISS Zen 3.0 software. The laser intensities are as follows: 405 nm, 17%; 488 nm, 7%; 561 nm, 7%; 642 nm, 5%.

Image quantification

Raw image files were used for further analysis using Imaris software (Version 9.0.1, Oxford Instruments). For each region of the hippocampus, nucleus accumbens, periaqueductal gray, amygdala, and arcuate nucleus, manual surface reconstruction was performed based on MOR-mCherry, S100β, GABA, and PV-positive signals. The parameters were: surface details: 0.39615 μm (smooth); diameter of the largest sphere: 1.4856 μm; color: base, diffusion transparency: 60% (0% for MOR surface). Then, we used the filter function on S100β, GABA, and PV surfaces to remove non-specific background signals and incomplete cells; filter: volume above 10.000 μm^3. After Imaris surface reconstruction, we counted MOR-positive and MOR-negative cell numbers based on S100β, GABA, or PV surface, using a cell counter plugin from the ImageJ program (NIH).

Virus injection

Mice were deeply anesthetized with vaporized isoflurane and immobilized in a stereotaxic (RWD Life Science). We targeted the CA1 region of the dorsal hippocampus (coordinates: AP -2 mm, ML±1.6 mm, DV -1.5 mm) for precise delivery of AAV-GFAP104-iGluSnfr virus (IBS Virus Facility). We administered 1 μl of the

https://doi.org/10.5607/en23039

virus at a rate of 0.2 μl/min and allowed 2~3 weeks for the AAV virus. AAV-GFAP104-iGluSnfr virus was bilaterally microinjected into the hippocampus CA1 of 7 to 9-week-old MOR-mCherry reporter mice.

Preparation of hippocampus and glutamate imaging

Glutamate sensor expressing MOR-mCherry reporter mice were deeply anesthetized with isoflurane, followed by decapitation. The brains were excised from the skull and placed in an ice-cold oxygenated cutting solution (250 sucrose; 26 $NaHCO_3$; 10 D(+)-glucose; 4 $MgCl_2$; 3 myo-inositol; 2.5 KCl; 2 sodium pyruvate; 1.25 NaH_2PO_4; 0.5 ascorbic acid; 0.1 $CaCl_2$; and 1 kynurenic acid (in mM), pH 7.4). After trimming the brain, coronal slices were cut 300-μm-thick in thickness with a vibrating microtome (PRO7N; DSK, Japan) and transferred in a chamber filled with oxygenated extracellular artificial cerebrospinal fluid (ACSF; 130 NaCl, 24 $NaHCO_3$, 3.5 KCl, 1.25 NaH_2PO_4, 1 $CaCl_2$, 3 $MgCl_2$ and 10 glucose (in mM), pH 7.4).

For glutamate imaging, brain slices were transferred to a recording chamber with a bath application of ACSF solution. The recording chamber was mounted on the stage of an upright microscope (Zeiss, Germany) and visualized with a CMOS camera (Hamamatsu, Japan). Image workbench (Indec biosystems) was utilized with a 60X water-immersion objective lens (numerical aperture: 0.9) and a 488-nm fluorescent imaging filter. Astrocytes were scanned at a rate of 0.5 frames per second during imaging sessions. DAMGO (1 μM), TTX (0.5 μM), and glutamic acid (1 mM) were bath applied.

RESULTS

Functional MOR expression in astrocytes of MOR-mCherry mice

To investigate the expression and proportion of astrocytic and neuronal MOR (*Oprm1*) in various brain regions, we utilized MOR-mCherry reporter mice [14]. In these mice, a reporter mCherry is tagged to the C-terminus of MOR (Fig. 1A) [14]. This reporter model offers the advantage of expressing MOR-mCherry under the native MOR promoter, ensuring endogenous levels of MOR with its native distribution pattern. Utilizing the advantages of the MOR-mCherry mouse model, which shows a high concentration of MOR-mCherry signals in key regions such as the temporal lobe (hippocampus, amygdala), basal forebrain (nucleus accumbens), hypothalamus (arcuate nucleus), and midbrain (periaqueductal gray region), we performed immunohistochemistry with cell-type-specific markers in these areas (Fig. 1B). We identified astrocytes using antibodies against S100β, and GABAergic inhibitory neurons using antibodies against GABA and parvalbumin (PV).

We have previously demonstrated through electron microscopy and immunogold labeling that MOR is highly expressed in the soma and processes of hippocampal astrocytes [17]. Similarly, we employed super-resolution lattice SIM imaging with the Zeiss Elyra 7 system in MOR-mCherry mice to confirm the expression of MOR-positive signals in the soma and processes of hippocampal astrocytes (Fig. 1C). Moreover, we observed a MOR-mCherry signal in the soma of GABAergic neurons, especially those positive for parvalbumin, a major subtype known to express MOR. These findings further corroborate the widespread and distinct expression of MOR in key neuronal and glial cell types within the brain.

Next, we asked whether the astrocytic MOR of MOR-mCherry mice functioned normally as previously demonstrated that astrocytic MOR releases glutamate [4, 5]. To examine this idea, we used virus-mediated expression of the glutamate sensor, iGluSnFr [18], selectively in the hippocampal astrocytes of MOR-mCherry mice using the GFAP promoter (Fig. 1D). We found that bath application of MOR agonist (1 μM), DAMGO, induced a glutamate signal in the astrocytes and the glutamate signal was not TTX-dependent (Fig. 1E), which was consistent with our previous findings in wild-type mice [4, 5]. At the same time, the glutamate sensor was confirmed by the application of glutamic acid (1 mM) (Fig. 1E). Taken together, these results indicate that MOR-mCherry mice can be effectively used to study MOR expression in astrocytes and other known regions like the hippocampus for comprehensive understanding of MOR distribution.

Hippocampus

Next, we investigate the population of MOR in the astrocytes and GABAergic neurons of the hippocampus. Using Imaris, we observed that astrocytic MOR is located in the membrane, forming puncta, while it covers almost the whole cell body of GABAergic neurons in the hippocampus CA1 (Fig. 2A). We found that 70.0% of S100β-positive astrocytes expressed MOR-mCherry positive signal (Fig. 2A, B), which was similar to the previous finding [17]. Moreover, we found that 93.0% of GABA-positive GABAergic neurons expressed MOR-mCherry in the hippocampus CA1 (Fig. 2A, B) as previously reported [19]. When only comparing the proportions of MOR-positive cells, we observed a higher percentage of MOR-positive cells among S100β-positive astrocytes (72.6%) compared to GABAergic neurons (27.4%), as indicated by the average cell number of S100β-positive cells (n=15.2) and GABAergic neurons (n=5.7) per image (Fig. 2C, D).

We then compared the expression of MOR in PV-positive cells, which are a primary source of somatic inhibition and GABAergic

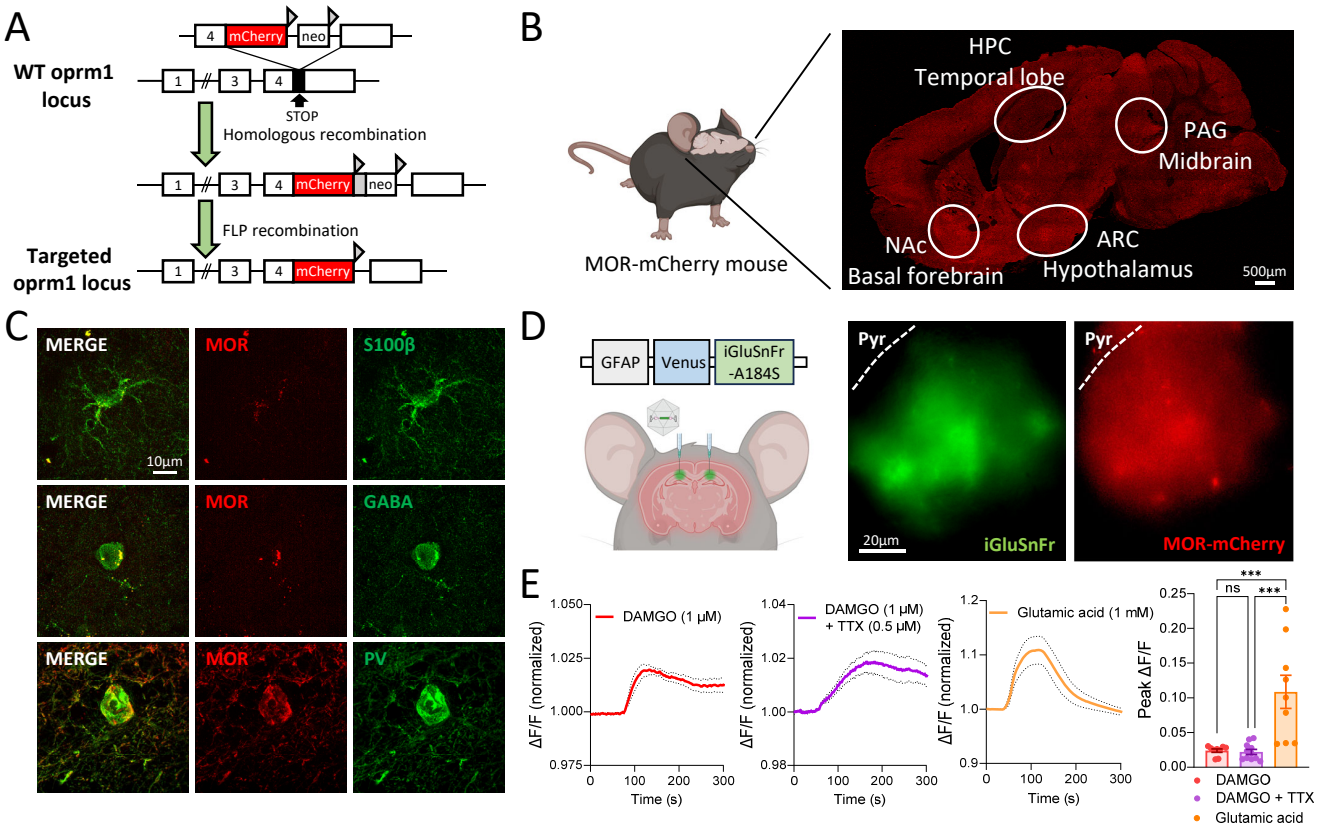

Fig. 1. Expression of functional MOR in the hippocampus of MOR-mCherry mice. (A) Schematic images of the construction of the MOR-mCherry reporter gene. (B) Expression pattern of MOR-associated mCherry in the various brain regions. (C) Representative SIM images of MOR-mCherry expressed in astrocytes, GABAergic neurons, and PV neurons of the hippocampus. (D) Representative images of iGluSnFr (glutamate sensor) and MOR-mCherry expression in the hippocampus of MOR-mCherry mice. (E) Summary traces of glutamate signal from iGluSnFr expressing astrocytes with an application of DAMGO (1 μM), TTX (0.5 μM), and glutamic acid (1 mM). Data are presented as the mean±s.e.m. ***p<0.001.

neurons [20]. We found that 88.9% of GABAergic neurons were PV-positive cells (Fig. 2E) and 90.8% of these cells were MOR-mCherry-positive (Fig. 2F, G). Also, we observed a higher portion of MOR-positive cells among S100β-positive astrocytes (77.6%, n=12.9) compared to PV-positive (22.4%, n=3.7) cells per image (Fig. 2H, I). Taken together, these results show that most astrocytes express MOR on their membrane as puncta, and almost all GABAergic and PV-positive neurons express MOR in the soma. In addition, these suggest that functional astrocytic MOR is predominant and outnumbers that in GABAergic neurons within the hippocampus.

Nucleus accumbens

We next investigated the proportion of astrocytic MOR in the nucleus accumbens, a brain region involved in the MOR-associated mesolimbic dopamine reward system [21, 22]. Our previous research suggested the presence of astrocytic MOR in the nucleus accumbens [17], but the proportion was not estimated. Therefore, we performed immunohistochemistry using antibodies against S100β, GABA, and PV in MOR-mCherry tissue samples and conducted a validation analysis using Imaris software. We confirmed the presence of astrocytic MOR as we suggested previously [17]. Furthermore, we observed that 62.4% of S100β-positive astrocytes expressed MOR-mCherry positive signals and 81.4% of GABAergic neurons exhibited MOR-cherry positive signals, indicating a high prevalence of MOR expression in both cell types within the nucleus accumbens (Fig. 3A, B). A closer examination of the cellular distribution showed a relatively balanced presence of MOR between S100β-positive astrocytes (55.5%, n=10.9) and GABAergic neurons (44.5%, n=8.7), indicating a similar distribution of MOR among these cells (Fig. 3C, D). Given the critical role of PV-positive neurons in the nucleus accumbens, particularly in feedforward inhibition, we delved further into the MOR-mCherry expression specifically within this neuronal subtype [22, 23]. We found that around half of GABAergic neurons were PV-positive cells (45.8%) and those PV-positive cells majorly displayed MOR-

 https://doi.org/10.5607/en23039

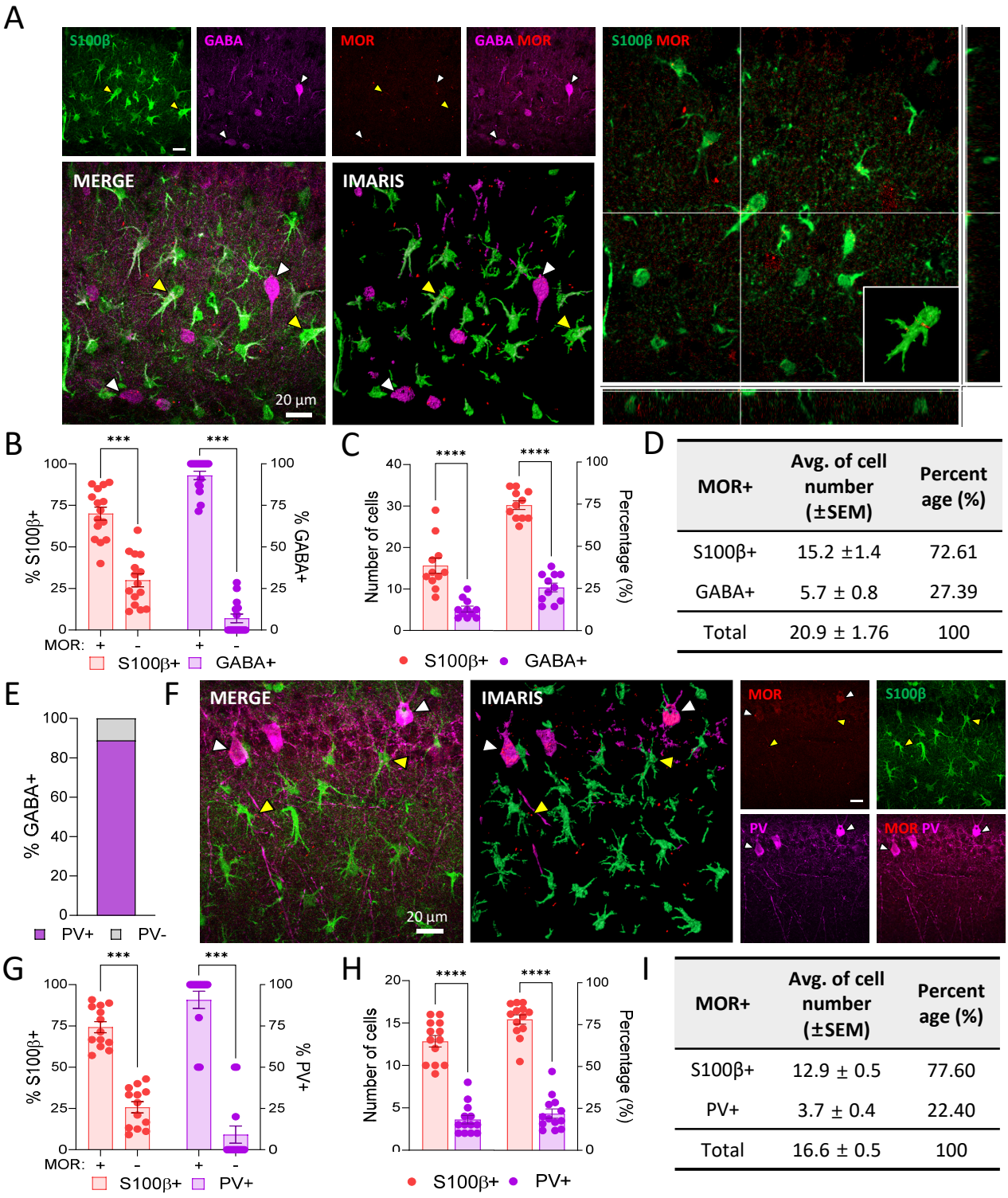

MOR+	Avg. of cell number (±SEM)	Percentage (%)
S100β+	15.2 ±1.4	72.61
GABA+	5.7 ± 0.8	27.39
Total	20.9 ± 1.76	100

MOR+	Avg. of cell number (±SEM)	Percentage (%)
S100β+	12.9 ± 0.5	77.60
PV+	3.7 ± 0.4	22.40
Total	16.6 ± 0.5	100

Fig. 2. MOR expression in the hippocampus. (A) Expression of MOR-mCherry, S100β, and GABA in the hippocampus of MOR-mCherry mice (yellow arrowheads indicate astrocytes; white arrowheads indicate GABAergic neurons). 3D rendering image was constructed with Imaris software. (B~D) Bar graph of S100β and GABA (B), number of cells and percentage of MOR positive cells (C), and summary table (D) in the hippocampus. (E) Bar graph of the percentage of PV positive cells in GABAergic neurons. (F) Expression of MOR-mCherry, S100β, and PV in the hippocampus of MOR-mCherry mice (yellow arrowheads indicate astrocytes; white arrowheads indicate PV neurons). 3D rendering image was constructed with Imaris software. (G~I) Bar graph of MOR population in S100β and PV (G), number of cells and percentage of MOR positive cells (H), and summary table (I) in the hippocampus. Data are presented as the mean±s.e.m. ***p<0.001, ****p<0.0001.

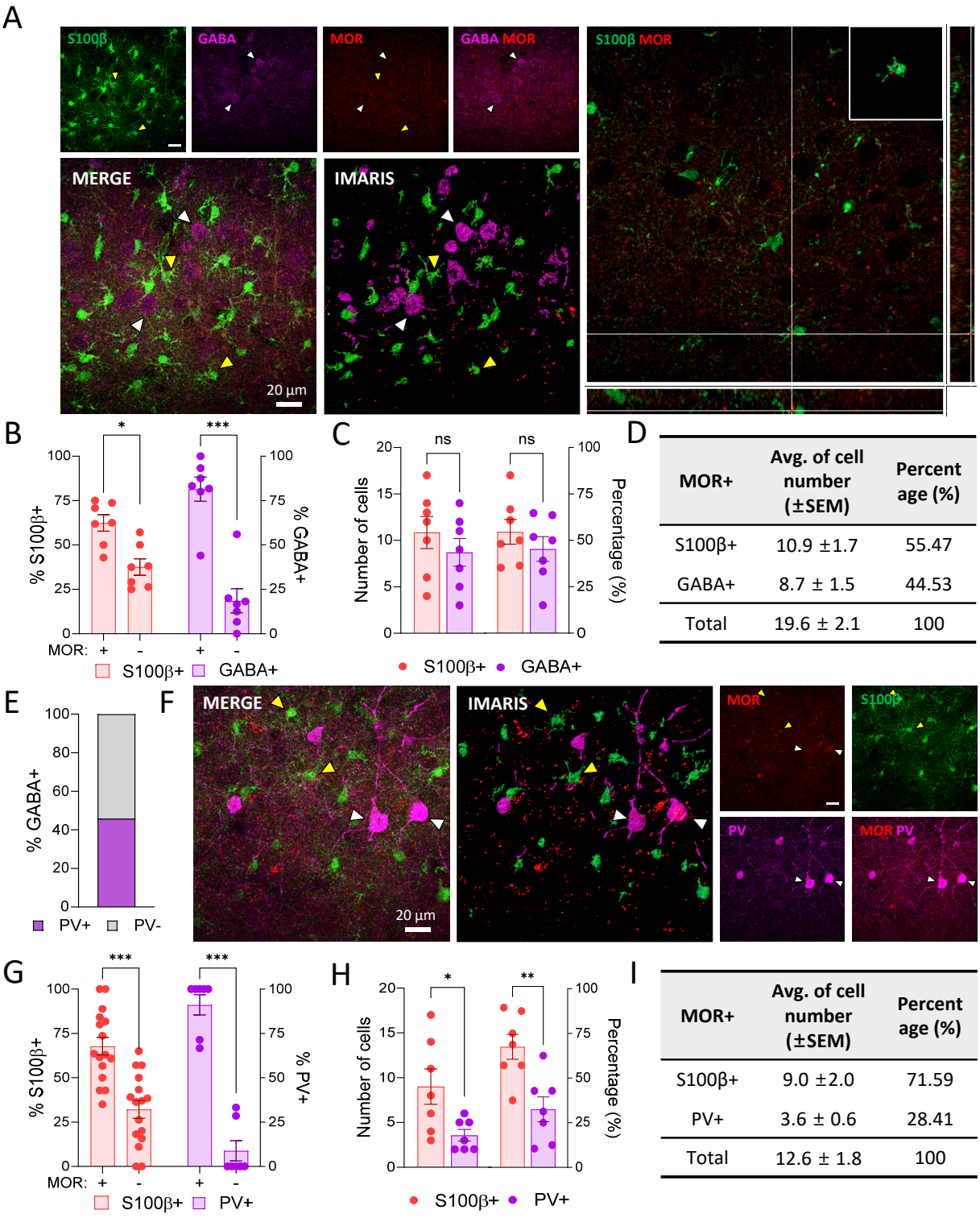

MOR+	Avg. of cell number (±SEM)	Percentage (%)
S100β+	10.9 ±1.7	55.47
GABA+	8.7 ± 1.5	44.53
Total	19.6 ± 2.1	100

MOR+	Avg. of cell number (±SEM)	Percentage (%)
S100β+	9.0 ±2.0	71.59
PV+	3.6 ± 0.6	28.41
Total	12.6 ± 1.8	100

Fig. 3. MOR expression in the nucleus accumbens. (A) Expression of MOR-mCherry, S100β, and GABA in the nucleus accumbens of MOR-mCherry mice (yellow arrowheads indicate astrocytes; white arrowheads indicate GABAergic neurons). 3D rendering image was constructed with Imaris software. (B~D) Bar graph of S100β and GABA (B), number of cells and percentage of MOR positive cells (C), and summary table (D) in the nucleus accumbens. (E) Bar graph of the percentage of PV positive cells in GABAergic neurons. (F) Expression of MOR-mCherry, S100β, and PV in the nucleus accumbens of MOR-mCherry mice (yellow arrowheads indicate astrocytes; white arrowheads indicate PV neurons). 3D rendering image was constructed with Imaris software. (G~I) Bar graph of S100β and PV (G), number of cells and percentage of MOR positive cells (H), and summary table (I) in the nucleus accumbens. Data are presented as the mean±s.e.m. *p<0.05, **p<0.01, ***p<0.001.

https://doi.org/10.5607/en23039

mCherry positivity (91.2%) (Fig. 3F, G). These findings not only affirm the previously noted expression patterns but also highlight a significant representation of MOR in the PV-positive neuron population. The expression ratio of MOR in S100β-positive astrocytes and PV-positive neurons was similar as we observed in the hippocampus.

However, when we compared S100β-positive astrocytes with PV-positive neurons, we noted that both the number and percentage in PV-positive cells (28.4%, n=3.6) were smaller than those in S100β-positive cells (71.6%, n=9.0) (Fig. 3H, I). Altogether, our findings suggest that the substantial expression of MOR in S100β-positive astrocytes in the nucleus accumbens and astrocytic MOR could be important as in GABAergic and PV-positive neurons.

Periaqueductal gray

We then examined whether MOR is present in the astrocytes of periaqueductal gray, which is reported to be involved in nociception modulation by MOR-meditated dopamine neuron synaptic transmission [24]. Similar to the hippocampus and nucleus accumbens, we analyzed MOR-mCherry positive signals in astrocytes. We found that S100β-positive astrocytes expressed a prominent MOR-mCherry signal in the periaqueductal gray, as well as GABAergic neurons (Fig. 4A, B). We observed that 68.7% of astrocytes exhibited expression of MOR-mCherry and 82.8% of GABAergic neurons expressed the MOR-mCherry signal (Fig. 4A, B). When only comparing the numbers and proportions of MOR-positive cells, we found a higher number and percentage of MOR-positive cells among S100β-positive astrocytes (59.9%) compared to GABAergic neurons (40.1%), based on the average cell numbers of S100β-positive cells (n=17.7) and GABAergic neurons (n=11.9) per image (Fig. 4C, D).

We next examined the MOR-mCherry signal in PV-positive neurons. Only 35.2% of the GABAergic neurons were identified as PV-positive (Fig. 4E). When investigating percentages of MOR-mCherry in PV-positive neurons, 64.3% of these cells were MOR-mCherry positive, but there was statistically no difference compared to the MOR-mCherry negative (Fig. 4F, G). Furthermore, upon comparing the ratios and numbers, we observed that S100β-positive astrocytes (71.0%, n=12.6) demonstrated a higher proportion compared to PV-positive cells (29.0%, n=5.1) (Fig. 4H, I). Altogether, these results suggest that MOR is also prominently expressed in astrocytes within the periaqueductal gray region.

Amygdala

In addition to other brain regions, MOR is also known to be expressed in GABAergic interneurons of the amygdala, which are associated with memory consolidation of aversive events, reward, and hyperphagia [25-27]. Although the amygdala shows the highest MOR binding density in the brain [27], the distribution of MOR, including astrocytes, remains unexplored. Thus, we next asked whether MOR is expressed in astrocytes of the amygdala. After analyzing the MOR-mCherry signal, we observed that 71.1% of astrocytes showed the presence of MOR-mCherry in the amygdala, while 80.5% of GABAergic neurons in the amygdala expressed MOR (Fig. 5A, B). Comparing cell numbers and proportions, we observed a similar pattern between S100β-positive astrocytes (46.8%, n=12.7) and GABAergic neurons (53.2%, n=14.4) in the amygdala, akin to the nucleus accumbens (Fig. 5C, D). Moreover, among the observed brain regions in this study, the amygdala exhibited the highest numbers and percentage of GABAergic neurons expressing MOR-mCherry (Fig. 5C, D).

Next, we examined the comparison of the MOR-mCherry signal between PV and S100β-positive cells. We found that 89.4% of GABAergic neurons were PV-positive (Fig. 5E). Among them, 61.0% were MOR-mCherry positive, although this ratio was found to be non-significant compared to the MOR-mCherry negative (Fig. 5G). When comparing cell numbers and proportions, PV (21.3%, n=3.6) exhibited relatively lower numbers and proportions compared to S100β-positive astrocytes (78.7%, n=13.4) (Fig. 5H, I). Altogether, these results suggest that in the amygdala, MOR-mCherry is also highly expressed in astrocytes.

Arcuate nucleus

MOR is also present in the arcuate nucleus, which plays a crucial role in energy homeostasis and neuroendocrine functions [26]. Despite the arcuate nucleus being a critical site for MOR activity, the specific distribution of astrocytic MOR is unknown. We found that 81.7% of MOR-mCherry was expressed in astrocytes, while 71.5% of the GABAergic neurons expressed MOR (Fig. 6A, B). In the case of cell number and proportion comparisons, we found that a total of 23 identified S100β-positive astrocytes comprising 72% of MOR-mCherry signals, as opposed to the 9 GABAergic neurons making up 27.9% (Fig. 6C, D). Notably, the arcuate nucleus displayed the greatest percentage of S100β-positive astrocytes for MOR-mCherry among the brain regions (Fig. 6C, D).

When focusing on the specific types of GABAergic neurons, we found that 76.0% of them were PV-positive (Fig. 6E). Further analysis of the MOR-mCherry signals in PV-positive cells revealed that 64.6% of the cells were MOR-positive (Fig. 6F, G). When comparing the number and expression of MOR between S100β-positive astrocytes and PV-positive neurons, we found that astrocytes have a significantly higher prevalence, with an average of 19 cells exhibiting MOR expression, making up 89% of the total observed. Conversely, PV-positive neurons with MOR expression average only 2

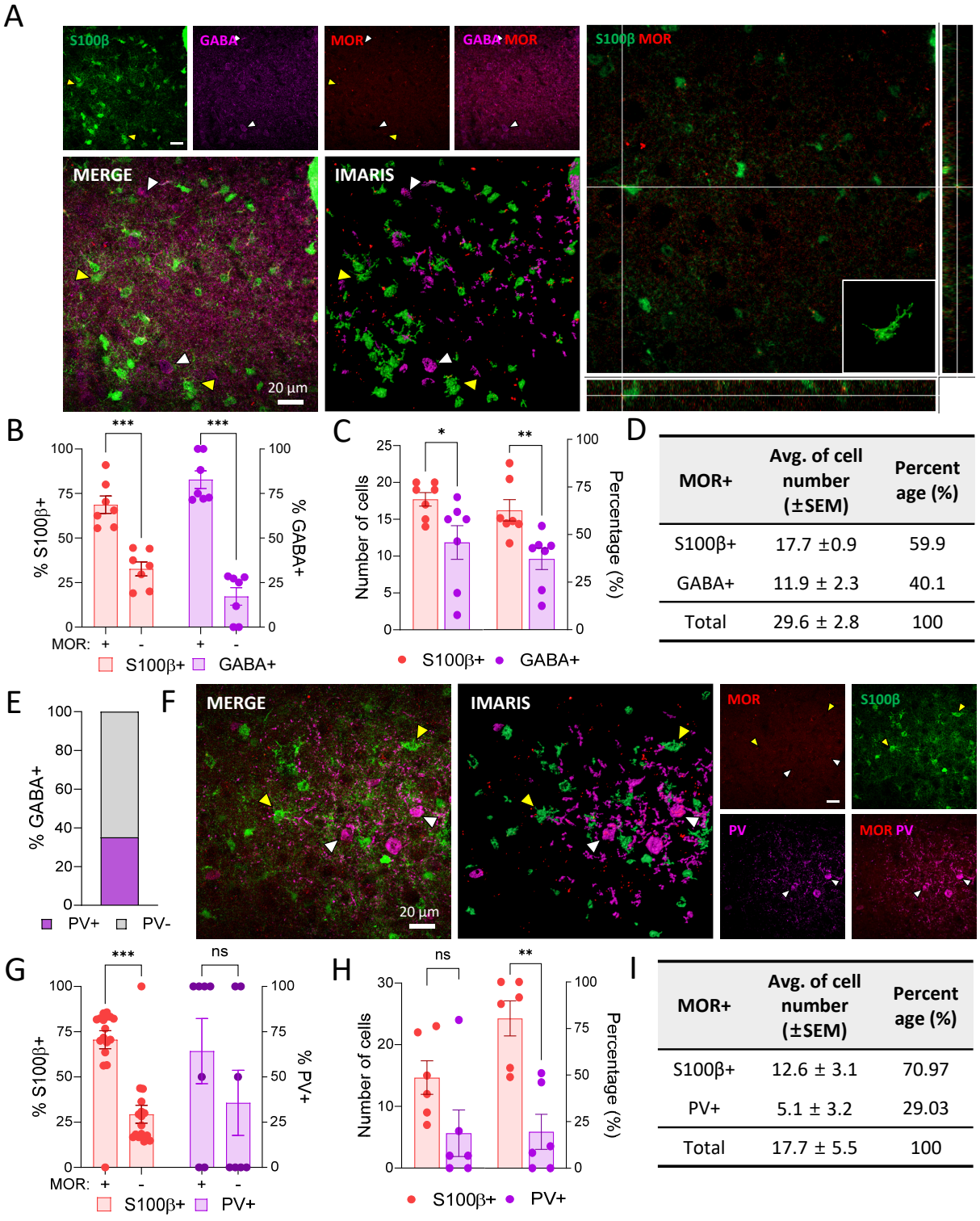

MOR+	Avg. of cell number (±SEM)	Percentage (%)
S100β+	17.7 ±0.9	59.9
GABA+	11.9 ± 2.3	40.1
Total	29.6 ± 2.8	100

MOR+	Avg. of cell number (±SEM)	Percentage (%)
S100β+	12.6 ± 3.1	70.97
PV+	5.1 ± 3.2	29.03
Total	17.7 ± 5.5	100

Fig. 4. MOR expression in the periaqueductal gray. (A) Expression of MOR-mCherry, S100β, and GABA in the periaqueductal gray of MOR-mCherry mice (yellow arrowheads indicate astrocytes; white arrowheads indicate GABAergic neurons). 3D rendering image was constructed with Imaris software. (B~D) Bar graph of S100β and GABA (B), number of cells and percentage of MOR positive cells (C), and summary table (D) in the periaqueductal gray. (E) Bar graph of the percentage of PV positive cells in GABAergic neurons. (F) Expression of MOR-mCherry, S100β, and PV in the periaqueductal gray of MOR-mCherry mice (yellow arrowheads indicate astrocytes; white arrowheads indicate PV neurons). 3D rendering image was constructed with Imaris software. (G~I) Bar graph of S100β and PV (G), number of cells and percentage of MOR positive cells (H), and summary table (I) in the periaqueductal gray. Data are presented as the mean±s.e.m. *p<0.05, **p<0.01, ***p<0.001.

https://doi.org/10.5607/en23039

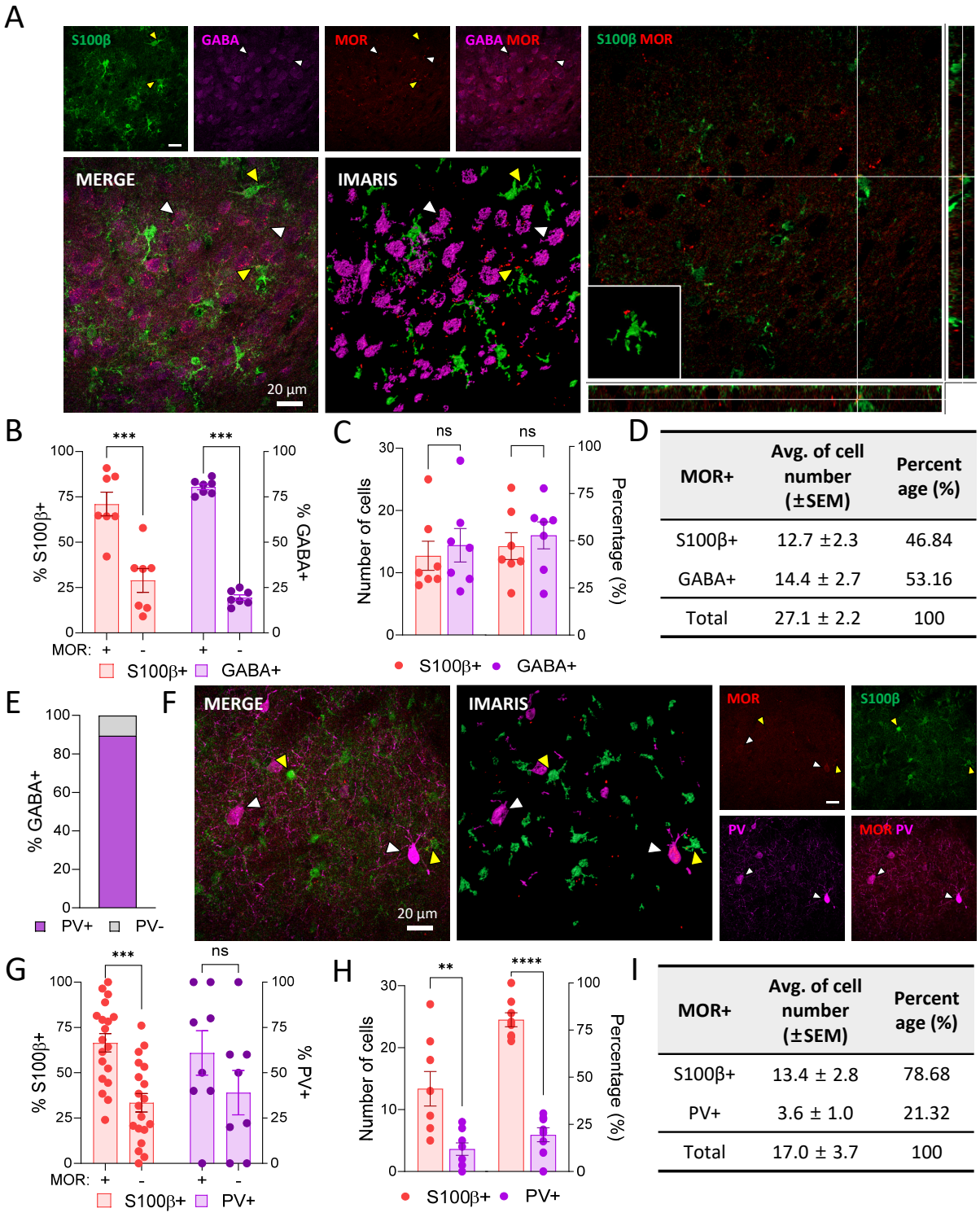

MOR+	Avg. of cell number (±SEM)	Percentage (%)
S100β+	12.7 ±2.3	46.84
GABA+	14.4 ± 2.7	53.16
Total	27.1 ± 2.2	100

MOR+	Avg. of cell number (±SEM)	Percentage (%)
S100β+	13.4 ± 2.8	78.68
PV+	3.6 ± 1.0	21.32
Total	17.0 ± 3.7	100

Fig. 5. MOR expression in the amygdala. (A) Expression of MOR-mCherry, S100β, and GABA in the amygdala of MOR-mCherry mice (yellow arrowheads indicate astrocytes; white arrowheads indicate GABAergic neurons). 3D rendering image was constructed with Imaris software. (B~D) Bar graph of S100β and GABA (B), number of cells and percentage of MOR positive cells (C), and summary table (D) in the amygdala. (E) Bar graph of the percentage of PV-positive cells in GABAergic neurons. (F) Expression of MOR-mCherry, S100β, and PV in the amygdala of MOR-mCherry mice (yellow arrowheads indicate astrocytes; white arrowheads indicate PV neurons). 3D rendering image was constructed with Imaris software. (G~I) Bar graph of S100β and PV (G), number of cells and percentage of MOR positive cells (H), and summary table (I) in the amygdala. Data are presented as the mean±s.e.m. **p<0.01, ***p<0.001, ****p<0.0001.

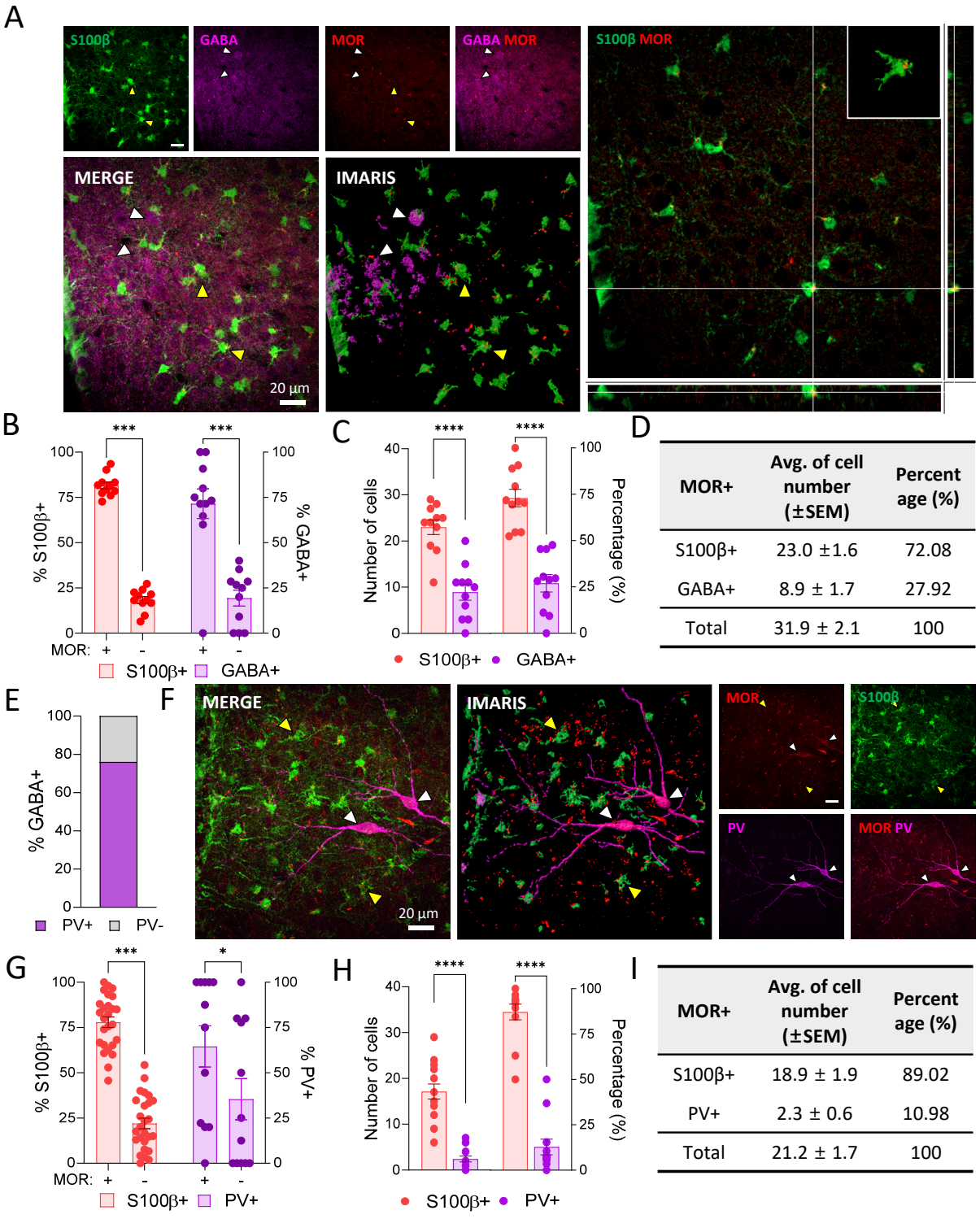

MOR+	Avg. of cell number (±SEM)	Percentage (%)
S100β+	23.0 ±1.6	72.08
GABA+	8.9 ± 1.7	27.92
Total	31.9 ± 2.1	100

I

MOR+	Avg. of cell number (±SEM)	Percentage (%)
S100β+	18.9 ± 1.9	89.02
PV+	2.3 ± 0.6	10.98
Total	21.2 ± 1.7	100

Fig. 6. MOR expression in the arcuate nucleus. (A) Expression of MOR-mCherry, S100β, and GABA in the arcuate nucleus of MOR-mCherry mice (yellow arrowheads indicate astrocytes; white arrowheads indicate GABAergic neurons). 3D rendering image was constructed with Imaris software. (B-D) Bar graph of S100β and GABA (B), number of cells and percentage of MOR positive cells (C), and summary table (D) in the arcuate nucleus. (E) Bar graph of the percentage of PV positive cells in GABAergic neurons. (F) Expression of MOR-mCherry, S100β, and PV in the arcuate nucleus of MOR-mCherry mice (yellow arrowheads indicate astrocytes; white arrowheads indicate PV neurons). 3D rendering image was constructed with Imaris software. (G-I) Bar graph of S100β and PV (G), number of cells and percentage of MOR positive cells (H), and summary table (I) in the arcuate nucleus. Data are presented as the mean±s.e.m. *p<0.05, ***p<0.001, ****p<0.0001.

https://doi.org/10.5607/en23039

cells, corresponding to 11% of the total observed (Fig. 6H, I). These results suggest that astrocytic MOR may have a significant role in energy homeostasis.

Sex-difference in the expression pattern of MOR

Neuronal MOR is known to exhibit sex-differences in expression and function: In the hippocampus and periaqueductal gray, a sex-dependent difference in MOR expression was observed, while a sex-dependent functional difference was found for MOR-dependent nociception and addiction [8, 10-12, 28, 29]. To investigate the sex-differences in the expression of astrocytic MOR in the various brain regions including the hippocampus, amygdala, and arcuate nucleus we compared the expression of MOR-mCherry signal in male and female mice (Fig. 7A~F). Among the various brain regions, we found that the amygdala showed the greatest sex-differences in the expression of MOR-mCherry signal in PV-positive neurons (male 32.5% vs. female 89.4%; difference 56.9%) (Fig. 7A, E). In the arcuate nucleus, females displayed higher levels of MOR-mCherry positive PV neurons compared to males (male 53.1% vs. female 87.5%; difference 34.4%) (Fig. 7F). However, we did not observe sex differences in astrocytic MOR expression across various brain regions, identifying only a non-significant trend in the hippocampus (Fig. 7B). These findings imply that the observed sex-dependent differences in MOR expression in the amygdala and arcuate nucleus are likely attributable to differences in MOR expression among PV-positive GABAergic neurons.

DISCUSSION

In this study, we have demonstrated the expression of astrocytic MOR in the various regions and quantified the proportion of S100β-positive astrocytic MOR compared to the GABAergic and PV-positive neurons via using MOR-mCherry reporter mice line, immunohistochemistry against cell-type specific antibodies, confocal super-resolution microscopy, and Imaris software. We revealed that MOR expression in astrocytes is not only prominent in the hippocampus (70.0%) as we previously shown [17], but also in other various brain regions including the nucleus accumbens (62.4%), periaqueductal gray (68.7%), amygdala (71.1%), and arcuate nucleus (78.0%) (Fig. 8). Interestingly, expression of astrocytic MOR in all selected MOR-related regions exceeded more than 60%. This outcome is also consistent with the results of in situ hybridization studies that identified astrocyte-specific oprm1 expression in the hippocampus, nucleus accumbens, and VTA [30]. As expected, in GABAergic neurons, expression of MOR was shown in the hippocampus (93.0%), nucleus accumbens (81.4%), periaqueductal gray (82.8%), amygdala (80.5%), and arcuate nucleus (71.5%) (Fig. 8). As for PV neurons, the order of high MOR expression was observed in the hippocampus (94.6%), nucleus accumbens (91.2%), arcuate nucleus (65%), periaqueductal gray (64.31%), and amygdala (61.0%) (Fig. 8). This pattern of expression aligns with a previous density distribution in MOR-mCherry mice [14]. Moreover, the number of cells and proportion of MOR was relatively larger in S100β-positive astrocytes compared to PV-positive neurons across the selected brain regions. Taken together, these results suggest the potential role of astrocytic MOR in these regions.

In addition, we confirmed that the astrocytic MOR in MOR-mCherry mice functions normally, as evidenced by the DAMGO-induced glutamate release in hippocampal astrocytes. This functional result is consistent with the previous evidence of intact MOR functionality in the MOR-mCherry reporter mouse which has shown normal expression, trafficking, TREK-1 colocalization, and MOR-mediated behavior responses [5, 14, 15].

We suggested the possibility that the expression of astrocytic MOR exhibits sex-differences in the brain regions. Several studies already demonstrated the sex-differences regarding the neuronal MOR in the brain, such as the amygdala and hippocampus [3, 29, 31]. Human PET imaging studies have reported a higher MOR signal in females, and also higher binding density of MOR has been shown in females compared to males using autoradiography [11, 32]. Also, considering the fluctuation of the morphine-induced analgesic effect across the ovarian cycle [10] and MOR trafficking in PV neurons regulated by ovarian hormones [9], sex differences might be owing to sex hormones. In line with these findings, we demonstrated a significantly higher expression of PV-positive neuronal MOR in the amygdala and arcuate nucleus of female MOR-mCherry reporter mice compared to males (Fig. 7). Contrary to initial expectations, the significant sex-differences in astrocytic MOR expression were not found across the various brain regions, and this trend was similarly observed in GABAergic neurons too. These results implicate that the PV-positive GABAergic MOR may be a major contributor to sex differences, while the astrocytic and PV-negative GABAergic MOR may be a minor contributor. Still, further research is needed to explore whether binding affinity or activity of astrocytic MOR varies depending on sex, focusing beyond just expression levels.

While the amygdala is known for fear consolidation, and emotion and exhibits the highest density of MOR according to receptor binding studies, the exact function of MOR is still elusive in this region [27]. In our previous study, we demonstrated that activation of astrocytic MOR in the hippocampus leads to the release of glutamate through the opening of TREK-1 channels [4, 5, 7]. Recent studies have shown that activating astrocytic MOR can

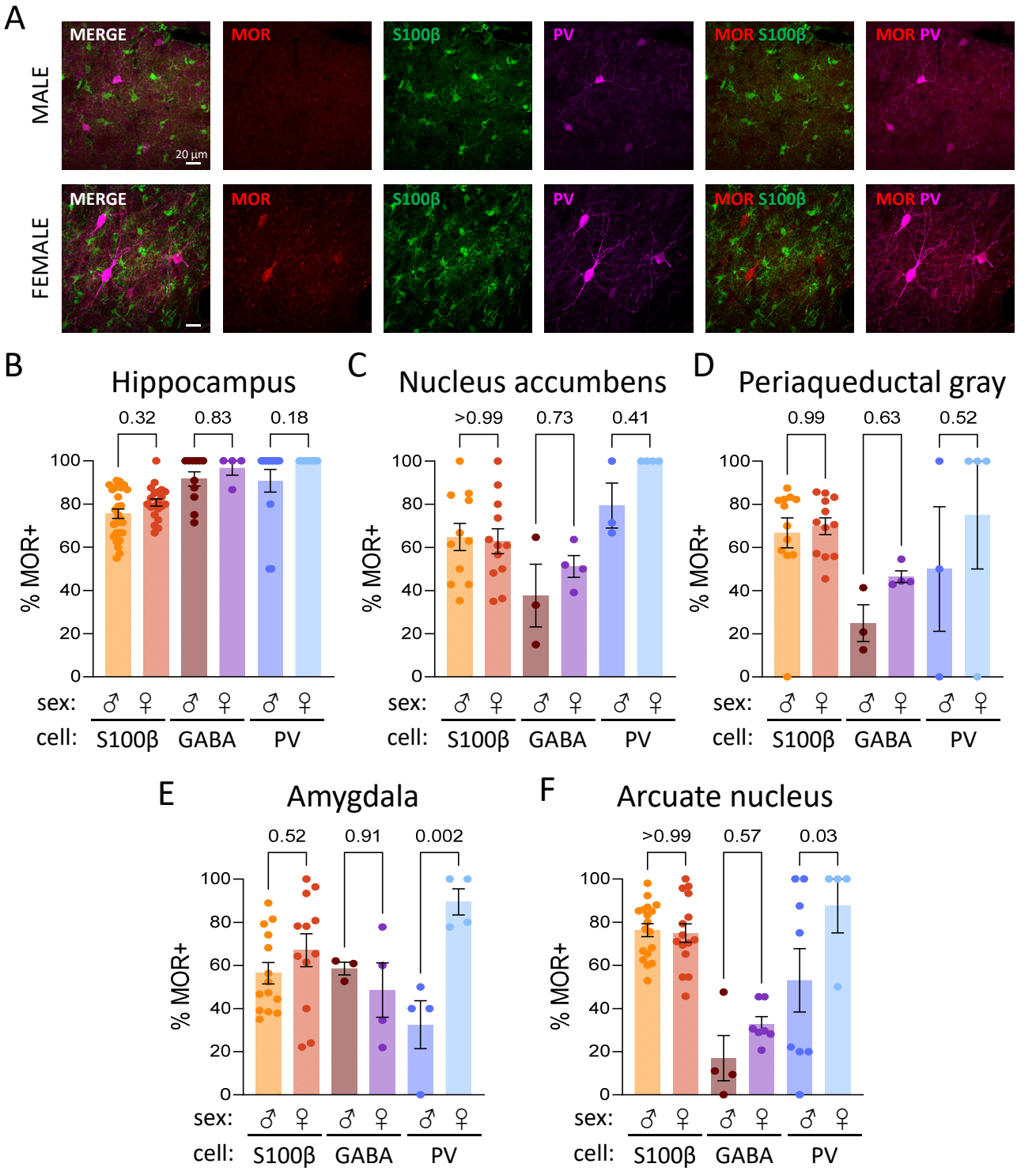

Fig. 7. Sex-dependent expression of MOR-mCherry. (A) Representative images of sex-dependent MOR expression in the amygdala. (B-F) The number of MOR-positive astrocytes, GABAergic neurons, and PV-positive neurons in the hippocampus (B), nucleus accumbens (C), periaqueductal gray (D), amygdala (E), and arcuate nucleus (F) from male (♂) and female (♀) MOR-mCherry mice.

rescue stress-induced anxiety [6, 33]. Moreover, TREK-1 is known to be markedly expressed in the various brain regions including the hippocampus, amygdala, nucleus accumbens, and hypothalamus [34]. Based on these findings, it would be interesting to test whether the activation of astrocytes through astrocytic MOR can cause glutamate release and rescue stress-induced anxiety or other

https://doi.org/10.5607/en23039

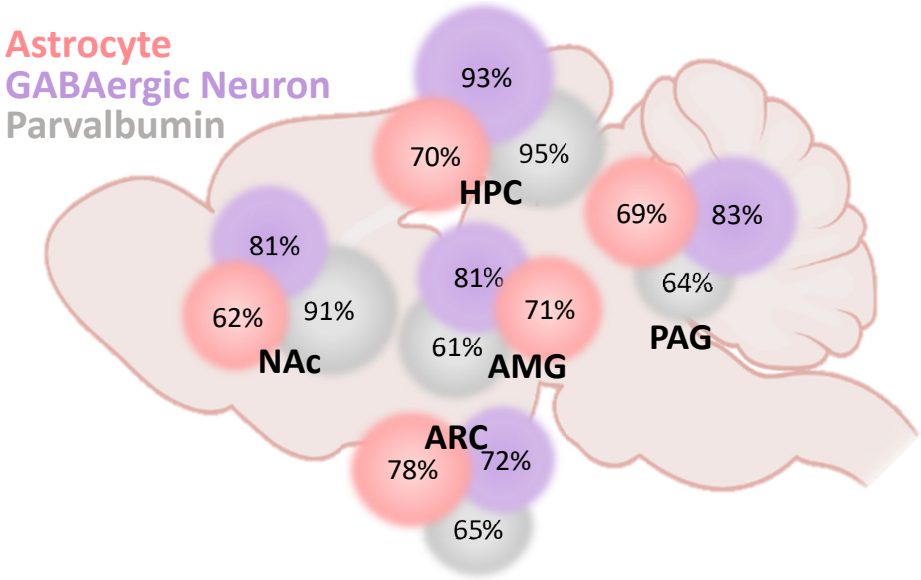

Fig. 8. Summary of MOR expression in the various brain regions of astrocytes, GABAergic neurons, and PV neurons (red, purple, and gray circles indicate the astrocytes, GABAergic neurons, and PV neurons, respectively; hippocampus, HPC; nucleus accumbens, NAc; periaqueductal gray, PAG; amygdala, AMG; arcuate nucleus, ARC).

amygdala-related behavior. Additionally, we aim to examine if activation of MOR interacts with TREK-1 and glutamate release in future investigations.

In conclusion, our findings unveil the robust expression of astrocytic MOR along with GABAergic or PV-positive neurons in the various MOR-dependent brain regions, including the hippocampus, arcuate nucleus, periaqueductal gray, amygdala, and nucleus accumbens. Also, this suggests a potential role for astrocytic MOR in modulating neuronal signaling and neurophysiological processes, highlighting the complex interplay between astrocytic and neuronal MOR, especially in PV-positive neurons.

ACKNOWLEDGEMENTS

This work was supported by the Institute for Basic Science (IBS), Center for Cognition and Sociality (IBS-R001-D2).

REFERENCES

1. Saidak Z, Blake-Palmer K, Hay DL, Northup JK, Glass M (2006) Differential activation of G-proteins by mu-opioid receptor agonists. Br J Pharmacol 147:671-680.
2. Valentino RJ, Volkow ND (2018) Untangling the complexity of opioid receptor function. Neuropsychopharmacology 43:2514-2520.
3. Nam MH, Won W, Han KS, Lee CJ (2021) Signaling mechanisms of μ-opioid receptor (MOR) in the hippocampus: disinhibition versus astrocytic glutamate regulation. Cell Mol Life Sci 78:415-426.
4. Nam MH, Han KS, Lee J, Won W, Koh W, Bae JY, Woo J, Kim J, Kwong E, Choi TY, Chun H, Lee SE, Kim SB, Park KD, Choi SY, Bae YC, Lee CJ (2019) Activation of astrocytic μ-opioid receptor causes conditioned place preference. Cell Rep 28:1154-1166.e5.
5. Woo DH, Bae JY, Nam MH, An H, Ju YH, Won J, Choi JH, Hwang EM, Han KS, Bae YC, Lee CJ (2018) Activation of astrocytic μ-opioid receptor elicits fast glutamate release through TREK-1-containing K2P channel in hippocampal astrocytes. Front Cell Neurosci 12:319.
6. Corkrum M, Rothwell PE, Thomas MJ, Kofuji P, Araque A (2019) Opioid-mediated astrocyte-neuron signaling in the nucleus accumbens. Cells 8:586.
7. Woo DH, Han KS, Shim JW, Yoon BE, Kim E, Bae JY, Oh SJ, Hwang EM, Marmorstein AD, Bae YC, Park JY, Lee CJ (2012) TREK-1 and Best1 channels mediate fast and slow glutamate release in astrocytes upon GPCR activation. Cell 151:25-40.
8. Milner TA, Burstein SR, Marrone GF, Khalid S, Gonzalez AD, Williams TJ, Schierberl KC, Torres-Reveron A, Gonzales KL, McEwen BS, Waters EM (2013) Stress differentially alters mu opioid receptor density and trafficking in parvalbumin-containing interneurons in the female and male rat hippocampus. Synapse 67:757-772.

9. Torres-Reveron A, Williams TJ, Chapleau JD, Waters EM, McEwen BS, Drake CT, Milner TA (2009) Ovarian steroids alter mu opioid receptor trafficking in hippocampal parvalbumin GABAergic interneurons. Exp Neurol 219:319-327.
10. Loyd DR, Murphy AZ (2014) The neuroanatomy of sexual dimorphism in opioid analgesia. Exp Neurol 259:57-63.
11. Smith CJW, Ratnaseelan AM, Veenema AH (2018) Robust age, but limited sex, differences in mu-opioid receptors in the rat brain: relevance for reward and drug-seeking behaviors in juveniles. Brain Struct Funct 223:475-488.
12. Wilson MA, Mascagni F, McDonald AJ (2002) Sex differences in delta opioid receptor immunoreactivity in rat medial amygdala. Neurosci Lett 328:160-164.
13. Quiñones-Jenab V, Jenab S, Ogawa S, Inturrisi C, Pfaff DW (1997) Estrogen regulation of mu-opioid receptor mRNA in the forebrain of female rats. Brain Res Mol Brain Res 47:134-138.
14. Erbs E, Faget L, Scherrer G, Matifas A, Filliol D, Vonesch JL, Koch M, Kessler P, Hentsch D, Birling MC, Koutsourakis M, Vasseur L, Veinante P, Kieffer BL, Massotte D (2015) A mu-delta opioid receptor brain atlas reveals neuronal co-occurrence in subcortical networks. Brain Struct Funct 220:677-702.
15. Zamfir M, Sharif B, Locke S, Ehrlich AT, Ochandarena NE, Scherrer G, Ribeiro-da-Silva A, Kieffer BL, Séguéla P (2023) Distinct and sex-specific expression of mu opioid receptors in anterior cingulate and somatosensory S1 cortical areas. Pain 164:703-716.
16. Maza N, Wang D, Kowalski C, Stoveken HM, Dao M, Sial OK, Giles AC, Grill B, Martemyanov KA (2022) Ptchd1 mediates opioid tolerance via cholesterol-dependent effects on μ-opioid receptor trafficking. Nat Neurosci 25:1179-1190.
17. Nam MH, Han KS, Lee J, Bae JY, An H, Park S, Oh SJ, Kim E, Hwang E, Bae YC, Lee CJ (2018) Expression of μ-opioid receptor in CA1 hippocampal astrocytes. Exp Neurobiol 27:120-128.
18. Marvin JS, Borghuis BG, Tian L, Cichon J, Harnett MT, Akerboom J, Gordus A, Renninger SL, Chen TW, Bargmann CI, Orger MB, Schreiter ER, Demb JB, Gan WB, Hires SA, Looger LL (2013) An optimized fluorescent probe for visualizing glutamate neurotransmission. Nat Methods 10:162-170.
19. Drake CT, Milner TA (2002) Mu opioid receptors are in discrete hippocampal interneuron subpopulations. Hippocampus 12:119-136.
20. Faget L, Erbs E, Le Merrer J, Scherrer G, Matifas A, Benturquia N, Noble F, Decossas M, Koch M, Kessler P, Vonesch JL, Schwab Y, Kieffer BL, Massotte D (2012) In vivo visualization of delta opioid receptors upon physiological activation uncovers a distinct internalization profile. J Neurosci 32:7301-7310.
21. Simmons D, Self DW (2009) Role of mu- and delta-opioid receptors in the nucleus accumbens in cocaine-seeking behavior. Neuropsychopharmacology 34:1946-1957.
22. Warren BL, Whitaker LR (2018) Parvalbumin-expressing neurons in the nucleus accumbens: a new player in amphetamine sensitization and reward. Neuropsychopharmacology 43:929-930.
23. Chen X, Liu Z, Ma C, Ma L, Liu X (2019) Parvalbumin interneurons determine emotional valence through modulating accumbal output pathways. Front Behav Neurosci 13:110.
24. Li C, Sugam JA, Lowery-Gionta EG, McElligott ZA, McCall NM, Lopez AJ, McKlveen JM, Pleil KE, Kash TL (2016) Mu opioid receptor modulation of dopamine neurons in the periaqueductal gray/dorsal raphe: a role in regulation of pain. Neuropsychopharmacology 41:2122-2132.
25. Liberzon I, Zubieta JK, Fig LM, Phan KL, Koeppe RA, Taylor SF (2002) μ-Opioid receptors and limbic responses to aversive emotional stimuli. Proc Natl Acad Sci U S A 99:7084-7089.
26. Barnes MJ, Primeaux SD, Bray GA (2008) Food deprivation increases the mRNA expression of micro-opioid receptors in the ventral medial hypothalamus and arcuate nucleus. Am J Physiol Regul Integr Comp Physiol 295:R1385-R1390.
27. Zhang J, Muller JF, McDonald AJ (2015) Mu opioid receptor localization in the basolateral amygdala: an ultrastructural analysis. Neuroscience 303:352-363.
28. Mills RH, Sohn RK, Micevych PE (2004) Estrogen-induced mu-opioid receptor internalization in the medial preoptic nucleus is mediated via neuropeptide Y-Y1 receptor activation in the arcuate nucleus of female rats. J Neurosci 24:947-955.
29. Nummenmaa L, Jern P, Malén T, Kantonen T, Pekkarinen L, Lukkarinen L, Sun L, Nuutila P, Putkinen V (2022) μ-Opioid receptor availability is associated with sex drive in human males. Cogn Affect Behav Neurosci 22:281-290.
30. Murlanova K, Jouroukhin Y, Novototskaya-Vlasova K, Huseynov S, Pletnikova O, Morales MJ, Guan Y, Kamiya A, Bergles DE, Dietz DM, Pletnikov MV (2023) Loss of astrocytic μ opioid receptors exacerbates aversion associated with morphine withdrawal in mice: role of mitochondrial respiration. Cells 12:1412.
31. Loyd DR, Wang X, Murphy AZ (2008) Sex differences in micro-opioid receptor expression in the rat midbrain periaqueductal gray are essential for eliciting sex differences in

morphine analgesia. J Neurosci 28:14007-14017.
32. Zubieta JK, Dannals RF, Frost JJ (1999) Gender and age influences on human brain mu-opioid receptor binding measured by PET. Am J Psychiatry 156:842-848.
33. Xiao Q, Xu X, Tu J (2020) Chronic optogenetic manipulation of basolateral amygdala astrocytes rescues stress-induced anxiety. Biochem Biophys Res Commun 533:657-664.
34. Djillani A, Mazella J, Heurteaux C, Borsotto M (2019) Role of TREK-1 in health and disease, focus on the central nervous system. Front Pharmacol 10:379.